Photorefractivity in Nematic Liquid Crystals Containing Electron Donor−Acceptor Molecules That Undergo Intramolecular Charge Separation

Gary P. Wiederrecht,*,† Beth A. Yoon,‡ Walter A. Svec,† and Michael R. Wasielewski*,†,‡

Contribution from the Chemistry Division, Argonne National Laboratory, Argonne, Illinois 60439, and Department of Chemistry, Northwestern University, Evanston, Illinois 60208

Received November 4, 1996[⊗]

Abstract: We report photorefractivity in nematic liquid crystals doped with electron donor−acceptor molecules that undergo intramolecular photoinduced charge separation. We show that subsequent intermolecular electron transfer from the intramolecular ion pairs to neutral donor−acceptor molecules is responsible for the charge migration over macroscopic distances that is required to produce photorefractivity. The results are compared to nematic liquid crystals doped with identical unlinked donors and acceptors that can achieve charge separation only through intermolecular electron transfer. We find that the liquid crystals doped with molecules that first undergo intramolecular charge separation exhibit superior photorefractivity when compared to the same liquid crystals doped with unlinked donors and acceptors. The differing mechanisms for charge generation and charge transport in these liquid crystal composites are analyzed.

Introduction

Liquid crystalline materials are of interest for a variety of applications in the areas of optical signal processing and photoinduced charge transport.[1−4] An exciting recent development is the marriage of both of these areas in nematic liquid crystals to produce photorefractive holograms.[5−8] The photorefractive effect holds great promise for reversible optical holography, noise-free optical image amplification, phase conjugate mirrors, and other optical signal processing techniques.[8−15] Photorefractivity is a light-induced change in the refractive index of a material. The mechanism for the refractive index change begins with a sample that weakly absorbs a laser beam. An appropriate sample will allow the absorbing chromophores to dissipate some of their energy through charge separation. Photovoltaic materials, or the application of an electric field, permit photoinduced directional charge transport over macroscopic distances. If the positive and negative charges have different mobilities, an electric field (or space charge field) is formed which modulates the index of refraction through either the linear or quadratic electrooptic effect. Clearly, the maximization of the photorefractive effect is not an easy problem, because the electrooptic, charge generation, charge transport, and charge trapping characteristics of a material must be simultaneously optimized. Furthermore, the absorbing chromophore must be tuned to match the laser wavelength for the application desired. For example, the chromophore utilized for optical signal processing applications at near-infrared telecommunications wavelengths will be different than the chromophore used for data storage applications in the blue region of the spectrum.

Nematic liquid crystals are novel photorefractive materials because their refractive index change is derived entirely from the quadratic electrooptic effect. Although this effect is usually associated with the high-temperature centrosymmetric phase of inorganic ferroelectric crystals,[16−18] the scope of this effect has become much broader with the recent advent of photorefractive polymers.[19−25] By decreasing the glass transition temperature of the host polymer, large increases in photorefractive gain are observed that cannot be explained by the linear electrooptic effect.[20−22] The enhancement is due to an ordering of the

† Argonne National Laboratory.

‡ Northwestern University.

⊗ Abstract published in *Advance ACS Abstracts,* March 15, 1997.

(1) Khoo, I. C. *Liquid Crystals: Physical Properties and Nonlinear Optical Phenomena*; Wiley: New York, 1995.

(2) Fekete, D.; AuYeung, J.; Yariv, A. *Opt. Lett.* **1980,** *5,* 51.

(3) Chen, A. G.; Brady, D. J. *Opt. Lett.* **1992,** *17,* 441.

(4) Adam, D.; Schuhmacher, P.; Simmerer, J.; Haussling, L.; Siemensmeyer, K.; Etzbach, K. H.; Ringsdorf, H.; Haarer, D. *Nature* **1994,** *371,* 141.

(5) Rudenko, E. V.; Sukhov, A. V. *JETP Lett.* **1994,** *59,* 142.

(6) Khoo, I. C.; Li, H.; Liang, Y. *Opt. Lett.* **1994,** *19,* 1723.

(7) Wiederrecht, G. P.; Yoon, B. A.; Wasielewski, M. R. *Science* **1995,** *270,* 1794.

(8) Wiederrecht, G. P.; Yoon, B. A.; Wasielewski, M. R. *Adv. Mater.* **1996,** *8,* 535.

(9) Gunter, P., Huignard, J.-P., Eds. *Photorefractive Materials and Their Applications I and II*; Springer-Verlag: Berlin, 1988.

(10) Feinberg, J. *Phys. Today* **1988,** *41,* 46.

(11) Feinberg, J.; Hellwarth, R. W. *Opt. Lett.* **1980,** *5,* 519.

(12) White, J. O.; Yariv, A. *Appl. Phys. Lett.* **1980,** *37,* 5.

(13) Shamir, J.; Caulfield, H. J.; Hendrickson, B. M. *Appl. Opt.* **1988,** *27,* 2912.

(14) Anderson, D. Z.; Lininger, D. M.; Feinberg, J. *Opt. Lett.* **1987,** *12,* 123.

(15) Nolte, D. D.; Olson, D. H.; Doran, G. E.; Knox, W. H.; Glass, A. M. *J. Opt. Soc. Am. B* **1990,** *7,* 2217.

(16) Chen, F. S. *J. Appl. Phys.* **1967,** *38,* 3418.

(17) von der Linde, D.; Glass, A. M.; Rodgers, K. F. *Appl. Phys. Lett.* **1975,** *26,* 155.

(18) Orlowski, R.; Boatner, L. A.; Kratzig, E. *Opt. Commun.* **1980,** *35,* 45.

(19) Ducharme, S.; Scott, J. C.; Twieg, J.; Moerner, W. E. *Phys. Rev. Lett.* **1991,** *66,* 1846.

(20) Moerner, W. E.; Silence, S. M. *Chem. Rev.* **1994,** *94,* 127.

(21) Meerholz, K.; Volodin, B. L.; Sandalphon; Kippelen, B.; Peyghambarian, N. *Nature* **1994,** *371,* 497.

(22) Meerholz, K.; Kippelen, B.; Peygambarian, N. *The Spectrum* **1995,** *8,* 1.

(23) Liphard, M.; Goonesekera, A.; Jones, B. E.; Ducharme, S.; Takacs, J. M.; Zhang, L. *Science* **1994,** *263,* 367.

(24) Zhang, Y.; Cui, Y.; Prasad, P. N. *Phys. Rev. B* **1992,** *46,* 9900.

(25) Yu, L.; Chan, W.; Bao, Z.; Cao, S. C. F. *J. Chem. Soc., Chem. Commun.* **1992,** 1735.

birefringent NLO chromophores within the space-charge field. For the most recent photorefractive polymers, the quadratic electrooptic (or orientational enhancement) effect has been shown to be responsible for a majority of the photorefractive gain.[22] One of the motivations for this work is that the orientational enhancement effect should be very large in liquid crystals due to their birefringent nature and the fact that they can reorient even within optical fields.[5]

In order to observe photorefractivity in nematic liquid crystals, they must first be doped with electron donors and/or acceptors that induce photoconductivity. This was initially accomplished by doping a nematic liquid crystal with dye molecules such as rhodamine 6G.[5,6] These dopants were limited by solubility and poor charge generation characteristics. We recently showed that by doping a eutectic mixture of nematic liquid crystals with electron donors and acceptors that have favorable redox properties, facile intermolecular charge transfer occurs, and a large photorefractive gain is observed.[7,8] A limitation of these composites is that the charge generation efficiency is limited by the excited state lifetime of the absorbing electron-donating chromophore. It must collide with an electron acceptor during its lifetime or no charge generation will occur. However, it is known that the lifetimes of intramolecular ion pairs are increased by a thousand times or more in liquid crystals.[26] We now report photorefractivity in liquid crystals that are doped with electron donor−acceptor molecules that undergo efficient photoinduced *intramolecular* charge separation. Since the observation of photorefractivity in liquid crystals relies on migration of charges over several microns, we show that the initial intramolecular charge separation is followed by intermolecular charge separation that results in bulk charge migration. The magnitude of the observed photorefractivity is found to be a function of the lifetime of the intramolecular charge separated state. We further show that intramolecular charge transfer dopants provide a more efficient mechanism for producing photorefractivity than intermolecular charge transfer dopants. This permits lower dopant concentrations that in turn reduce absorption losses in these materials.

Experimental Section

The experimental apparatus uses two coherent beams from an Ar$^+$ laser at 457 nm that are crossed in the sample as illustrated in Figure 1. Since the experiment is performed in the Raman−Nath (thin) grating regime, multiple diffracted beams are observed. Photorefractivity manifests itself as a gain in the diffracted and undiffracted intensity of one beam and a corresponding loss in the intensity of the other beam and its corresponding diffracted beams. The diffraction efficiency η is defined as the ratio of the energy in the first-order diffracted beam divided by the incident energy of the zero-order beam. As many as eight diffracted orders have been observed. The beams are unfocussed and have a $1/e$ diameter at the sample of 2.5 mm. The samples consist of 35% by weight 4′-(octyloxy)-4-biphenylcarbonitrile (**8OCB**) and 65% 4′-pentyl-4-biphenylcarbonitrile (**5CB**). The samples are homeotropically aligned by treatment of the ITO slides with octadecyltrichlorosilane.[1] The **8OCB/5CB** mixture lowers the nematic-to-solid phase transition from 24 °C for pure **5CB** to 5 °C.[27] We found superior photorefractivity for this mixture, presumably due to a greater reorientation angle of the molecules derived from a lower orientational viscosity of the liquid crystal mixture relative to **5CB**. The birefringence of **8OCB** is also slightly higher than that of **5CB**.[28] Additionally, neither component possesses any visible absorption, reducing unwanted competition with the charge generator for photons. The samples used
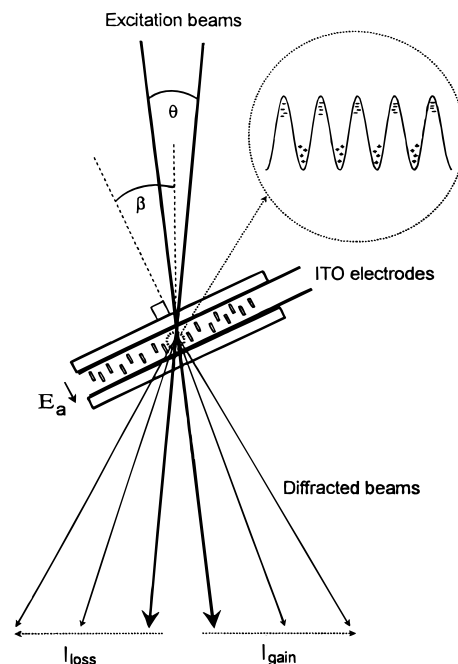

Figure 1. A schematic of the experimental geometry is illustrated. The sample is tilted at an angle $\beta = 30°$ relative to the bisector of the two beams. This allows for charge migration along the grating wavevector which results in a sinusoidal space charge field. A phase grating results from the influence of the electric field on the orientational configuration of the birefringent liquid crystal molecules. The beams are polarized in the plane of the paper (i.e. extraordinary) and parallel to the grating wavevector.

were 37 μm thick, as determined by a Teflon spacer. A low voltage power supply was utilized to apply voltages of up to 3 V to the sample, which resulted in electric fields of up to 0.81 kV/cm.

Four molecules (**1**−**4**) were utilized as the intramolecular charge transfer dopants. Their synthesis is described elsewhere.[29] They were chosen for the following reasons: (1) The lifetimes of the charge separated states in degassed toluene for **1**−**4** are 5.3, 104, 150, and 300 ns, respectively, as determined by time resolved transient absorption experiments.[29−31] As Table 1 illustrates, this trend is preserved in the liquid crystalline environment, with the lifetimes of the ion pairs increasing by at least one order of magnitude in the anisotropic solvent. This variation permits the study of photorefractivity as a function of the lifetime of the intramolecular charge separated state. (2) They undergo intramolecular charge separation with nearly 100% quantum yield. (3) Photoinduced electron transfer occurs through excitation of the 400 nm absorption bands of the donor chromophores based on the aminonaphthalene−dicarboximide derivatives. The tails of the dopants' absorption bands extend to at least 500 nm, which permits the use of an Ar$^+$ laser. Figure 2a illustrates the ground state absorption spectra of the donor and acceptor for both the intramolecular and intermolecular charge transfer dopants in toluene. The spectra are similar for all of the dopants, with the exception of **2**, which has a 50 nm red-shifted absorption band. Figure 2b illustrates the broadened spectrum of **3** in the liquid crystalline environment. The extinction coefficients at 457 nm are approximately 1000 M^{-1} cm^{-1} for **4**, 2000 M^{-1} cm^{-1} for **1**, 5000 M^{-1} cm^{-1} for **3**, and 10000 M^{-1} cm^{-1} for **2**. (4) They are well characterized in liquid crystalline environments.[30] They are soluble and their long axes are known to align parallel to the director of the liquid crystal.

Samples containing **1**−**4** were compared to liquid crystalline composites containing only the donor chromophore **5** and to composites containing both donor molecule **5** and the acceptor **NI**. This permitted

(26) Hasharoni, K.; Levanon, H.; Garschmann, J.; Schubert, H.; Kurreck, H.; Mobius, K. *J. Phys. Chem.* **1995**, *99*, 7514.

(27) Collings, P. J. *Liquid Crystals: Nature's Delicate Phase of Matter*; Princeton University Press: Princeton, NJ, 1990.
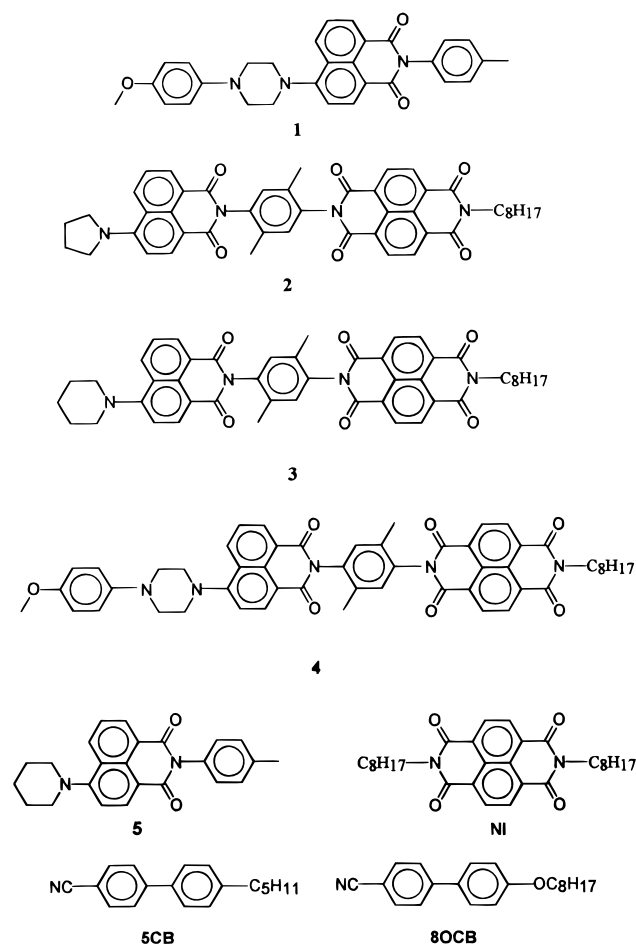
(28) Sen, S.; Brahma, P.; Roy, S. K.; Mukherjee, D. K.; Roy, S. B. *Mol. Cryst. Liq. Cryst.* **1983**, *100*, 327.

(29) Greenfield, S. R.; Svec, W. A.; Gosztola, D.; Wasielewski, M. R. *J. Am. Chem. Soc.* **1996**, *118*, 6767.

(30) Hasharoni, K.; Levanon, H.; Greenfield, S. R.; Gosztola, D. J.; Svec, W. A.; Wasielewski, M. R. *J. Am. Chem. Soc.* **1995**, *117*, 8055.

(31) Wiederrecht, G. P.; Watanabe, S.; Wasielewski, M. R. *Chem. Phys.* **1993**, *176*, 601.

Chart 1

Figure 2. (a) The ground state absorption spectra of **1**−**4** in toluene are illustrated. (b) The spectrum of **3** in a liquid crystalline environment is illustrated.

Table 1. The Charge Separation and Charge Return Constants in Toluene and the Liquid Crystal

	τ_{CS} toluene (ns)	τ_{CR} toluene (ns)	τ_{CR} LC (μs)
1	0.011	5.3	0.53
2	0.45	104	0.77
3	1.4	150	4.4
4	0.008	300	3.2

Table 2. The Free Energy for Charge Separation and Charge Return in Polar Liquids (Calculations are Made Assuming a Value for ϵ_s of 10.5)

	E_S (eV)	r_{12} (Å)	E_{OX} (eV)	E_{RED} (eV)	ΔG_{CS} (eV)	ΔG_{CR} (eV)
1	2.80	7.7	0.79	−1.41	−0.78	−2.02
2	2.48	15.2	1.08	−0.53	−0.96	−1.52
3	2.80	15.2	1.20	−0.53	−1.16	−1.64
4[a]	2.80	19.1	0.79	−1.41/−0.53	−0.78/−1.60	−1.17

[a] The charge separation in **4** occurs in two steps. The first step is photoinduced with energetics that are the same as in **1**, while the second thermal electron transfer produces the final, more distant ion pair.

a direct comparison of photorefractivity for systems in which the initial charge separation occurred through either an intermolecular or intramolecular mechanism. Compound **3** consists of a donor and an acceptor that are identical to **5/NI**.
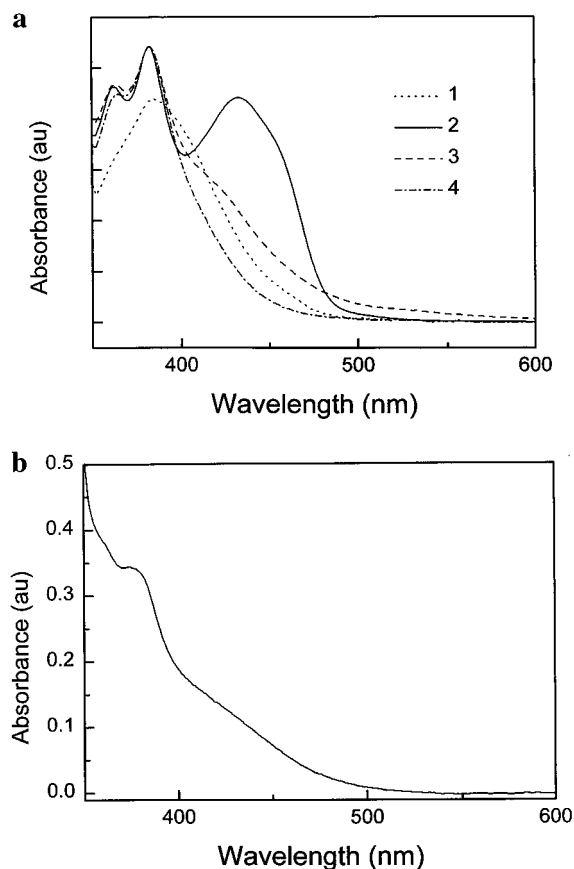
The excited states and free energies for charge separation are illustrated in Table 2. The free energy for charge separation (ΔG_{CS}) was calculated using the relationship:

$$\Delta G_{CS} = E_{OX} - E_{RED} - \frac{e_o{}^2}{\epsilon_s r_{12}} - E_s \qquad (1)$$

where E_{OX} is the oxidation potential of the donor, E_{RED} is the reduction potential of the acceptor, E_S is the first excited singlet state of the donor, e_o is the charge of an electron, ϵ_s is the static dielectric constant, and r_{12} is the center-to-center distance between the donor and acceptor.

Results

Figure 3 illustrates the asymmetric beam coupling that is the signature of photorefractive gratings. The diffraction pattern only appeared for extraordinary polarized light and with the application of an electric field. These observations confirm that the grating is due to an orientational photorefractive grating and not to thermal or absorption gratings.[5−8] A wavevector value

of $q = 1.1 \times 10^3$ cm^{-1}, corresponding to a fringe spacing $\Lambda = 57$ μm, was utilized for this measurement.

For quantitative comparison of the grating strengths in the different liquid crystal composites, the first-order diffraction efficiency measurements of the Raman-Nath gratings are reported. Several concentrations for each of the dopants were utilized, and Figure 4 illustrates the highest diffraction efficiency values vs applied voltage for the samples with the optimal concentration of each dopant. A wavevector value of $q = 1.1 \times 10^3$ cm^{-1} was again utilized. The first clearly noticeable fact is that the intramolecular charge transfer molecules **3** and **4** are superior to the intermolecular charge transfer dopants for inducing photorefractivity. For these dopants, larger diffraction efficiencies are achieved at lower applied fields. Photorefractivity for **3** is observed for an applied voltage as low as 0.2 V, corresponding to an applied field of only 50 V/cm. For applications purposes, **3** has superior chemical stability in the liquid crystals relative to **4**. Apparently, the methoxy group of **4** leads to photoinstability in the **5CB/8OCB** environment, which leads to a loss of photorefractivity over a few days. The voltages were not increased to higher values for these samples
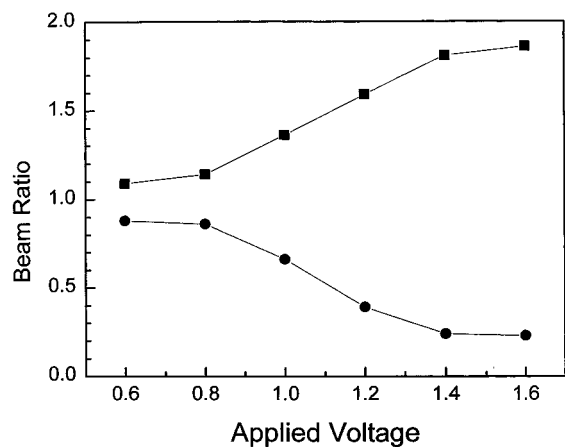
Figure 3. The asymmetric photorefractive beam coupling for a **5CB/8OCB** mixture containing 7.1×10^{-4} M of **3**, as measured by the ratio of the beam that gains (loses) intensity relative to its incident intensity, is illustrated.
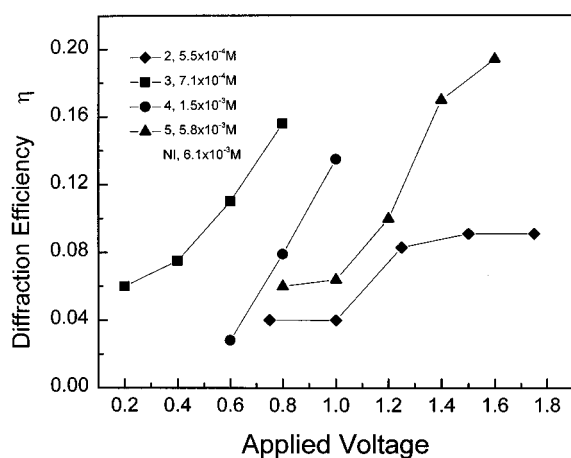

Figure 4. The diffraction efficiency of the photorefractive grating in the composite systems is illustrated. Note that high diffraction efficiency for the composites containing the intramolecular charge transfer dopants occurs at lower applied voltages than those for the intermolecular charge transfer dopants.

because the measurements were not found to be reliable for very strong gratings with numerous (>5) diffracted beams. Also, theories relating the diffraction efficiency of Raman-Nath gratings to various physical parameters are not valid for diffraction efficiencies above approximately 0.2.

The second point is that the magnitude of the diffraction efficiency for samples with intramolecular dopants **1**−**4** is clearly dependent upon the lifetime of the charge separated state. Dopant **1** has no measurable photorefractivity and a charge separated lifetime of only 530 ns in the liquid crystal. Dopant **2** has a charge separated lifetime of 770 ns and has diffraction efficiency comparable to that for samples doped with **5**. Liquid crystal composites containing dopants **3** and **4**, which have ion pair lifetimes of 4.4 and 3.2 μs, respectively, have dramatically increased photorefractivity over composites that contain dopants with shorter ion pair lifetimes.

The dependence of diffraction efficiency on the dopants' ion pair lifetime points to charge hopping as a mechanism for charge transport, because the likelihood that charges will hop to neighboring molecules increases with the lifetime of the charge separated state. Schemes 1 and 2 indicate the proposed mechanisms for bulk charge separation for composites containing intermolecular and intramolecular charge transfer dopants, respectively. Charge hopping in liquids has long been discussed as an enhancement mechanism for conduction in addition to

Scheme 1
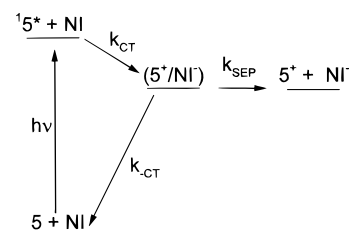
Scheme 2
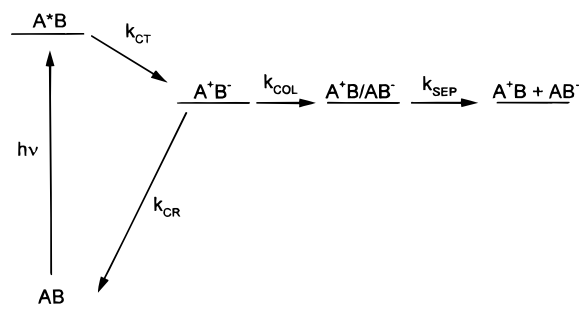
diffusion. For example, electron-exchange mechanisms were first discussed by Levich and Dahms.[32,33] Ruff and Friedrich generalized these theories and named the process "transfer diffusion".[34] This process has also been discussed in the framework of Marcus theory.[35]

The third important experimental observation is illustrated in Figure 5, which shows the diffraction efficiencies for the intramolecular and intermolecular charge transfer dopants as a function of concentration. Remarkably, the ideal concentration of the intramolecular dopant **3** is a factor of 6 less than that for the intermolecular case of **5/NI**, despite the fact that the identical chromophore is optically excited. Furthermore, in the concentration region studied, the intermolecular charge transfer samples displayed a monotonic increase in diffraction efficiency with concentration, whereas the intramolecular dopants actually showed lower diffraction efficiency at concentrations above approximately 1×10^{-3} M.

Discussion

The summary of the three important experimental observations is as follows: (1) Appropriate dopants which undergo intramolecular charge transfer are capable of providing large photorefractive grating diffraction efficiencies which exceed those for similar intermolecular charge transfer dopants. (2) The magnitude of the diffraction efficiency increases with longer ion pair lifetimes. (3) The concentration of dopants necessary to induce similar photorefractivity is significantly lower for the intramolecular charge transfer dopants than for the intermolecular charge transfer dopants. Additionally, the diffraction efficiency does not increase monotonically with concentration for the intramolecular charge transfer dopants as it does with the intermolecular charge transfer dopants. Thus, significantly lower concentrations and reduced absorption for the intramolecular ion pair dopants are achieved with superior photorefractive diffraction efficiency. These observations indicate important mechanistic differences for the production of bulk charge separation. An analysis of each of the above findings is made below.

(32) Levich, V. G. *Adv. Electrochem. Electrochem. Eng.* **1966**, *4*, 314.
(33) Dahms, H. *J. Phys. Chem.* **1968**, *72*, 362.
(34) Ruff, I.; Friedrich, V. *J. Phys. Chem.* **1971**, *75*, 3297.
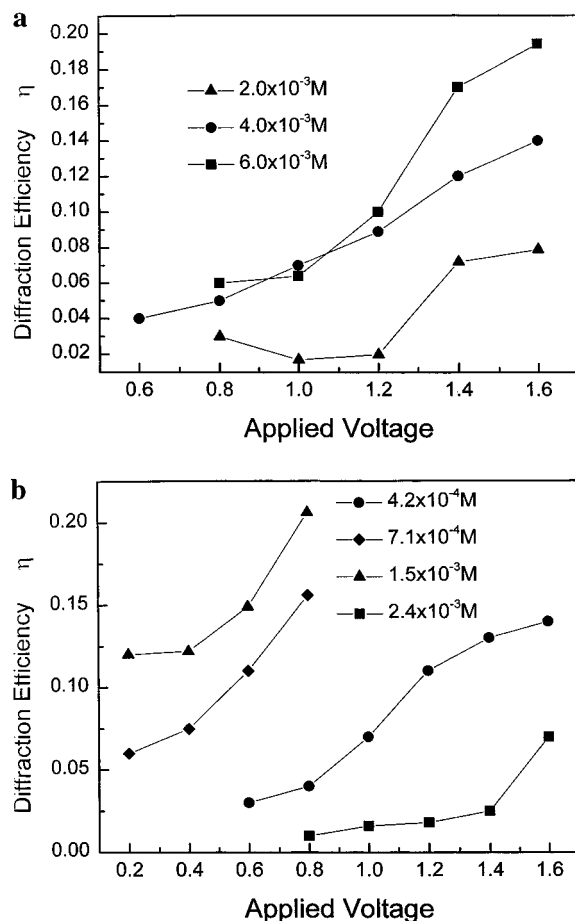(35) Suga, K.; Aoyagui, S. *Bull. Chem. Soc. Jpn.* **1973**, *46*, 755.

a

b

Figure 5. (a) The dependence of the diffraction efficiency vs concentration is illustrated for the composites containing the intermolecular charge transfer dopants **5/NI**. The concentrations of **5** and **NI** are equivalent and are given in the legend. A monotonic increase in diffraction efficiency with concentration is observed. (b) The dependence of the diffraction efficiency vs concentration is illustrated for the composites containing the intramolecular charge transfer dopant **3**. The diffraction efficiency is not a monotonic function of the concentration.

I. Superior Diffraction Efficiency for the Intramolecular Charge Transfer Dopants. As discussed in the introduction, photorefractivity can only occur if the mobility of the positive and negative charges are different. It is our goal in this section to show that the difference between the diffusion coefficients of the cations and anions is much larger for the intramolecular dopants vs the intermolecular dopants. The significance of this difference can be illustrated by the equation for a space charge field derived from ion diffusion with a light intensity modulation of $I = I_o(1 + \cos(\beta x))$:[5,9]

$$E_{SC} = \frac{-mk_BTq}{2e_o}\left(\frac{D^+ - D^-}{D^+ + D^-}\right)\left(\frac{\sigma_{ph}}{\sigma_{ph} + \sigma_d}\right)\sin(qx) \quad (2)$$

Here, σ_{ph} is the photoconductivity, σ_d is the dark conductivity, k_B is the Boltzmann constant, q is the wavevector of the grating, and D^+ and D^- are the diffusion constants for the cations and anions, respectively. Equal intensity beams are assumed. It is clear that the two factors which determine the magnitude of the space charge field are the difference in the photoconductivity versus dark conductivity and the difference between the diffusion coefficients of the cations and anions. These differences permit one set of charges to trap in the illuminated regions of the interference pattern and for the opposing charges to migrate into the nulls of the interference pattern before trapping.
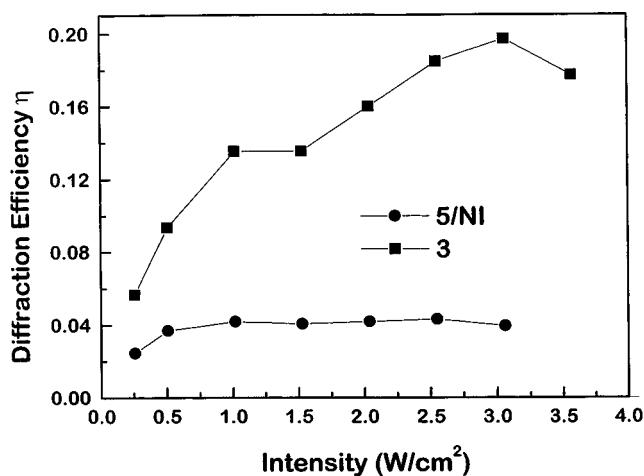

Figure 6. The diffraction efficiency of the photorefractive grating as a function of optical intensity is shown for composites containing either **3** or **5/NI**. The **5/NI** sample saturates at lower intensities than the composite containing **3**. The grating spacing is 16.9 μm.

We can determine the difference between the diffusion coefficients through the relation of these quantities to the diffraction efficiency η of a Raman-Nath orientational grating:[2,5]

$$\eta = \left(\frac{Lmk_BT}{\lambda n_e Kqe}\left(\frac{E_A\epsilon_s\epsilon_\infty \sin\beta}{1 + \dfrac{\epsilon E_A}{2\pi Kq^2}}\right)\left(\frac{\sigma_{ph}}{\sigma_{ph} - \sigma_d}\right)\nu\right)^2 \quad (3)$$

where $\nu = (D^+ - D^-)/(D^+ + D^-)$, L is the thickness of the sample, λ is the optical wavelength, n_e is the index of refraction along the extraordinary axis, K is the single constant approximation of the Frank elastic constant,[1,5] and ϵ_∞ is the high-frequency dielectric constant. Fortunately, the only variables that are a function of the dopants are the diffusion (ν) and conductivity terms. It has been previously shown that at higher light intensities, the conductivity term will saturate as $\sigma_{ph} \gg \sigma_d$.[5] Therefore, the value of ν can be determined for the different samples as long as the conductivity term is saturated. Figure 6 illustrates a plot of η as a function of intensity for samples with dopant **3** (7.1×10^{-4} M) and **5/NI** (both have concentrations of 5.8×10^{-3} M). The values of η in the saturation limit are different by a factor of 5, indicating that ν is much larger for the sample doped with **3** relative to that doped with **5/NI**. By using the values $K = 7 \times 10^{-7}$ dyn,[1] $\epsilon_\infty = 2.25$, $\epsilon_s = 10.5$, and $T = 298$ K, we obtain values for $\nu = 0.29$ for the composite containing **3** and $\nu = 0.04$ for the samples containing **5/NI**.[36] Thus, the values for ν show conclusively that the difference in the diffusion coefficients is much larger for the intramolecular charge transfer dopants relative to the intermolecular charge transfer dopants. Furthermore, these results compare very favorably to the value of $\nu = 0.02$ reported for R6G in **5CB**.[5]

The absolute value for the diffusion coefficients of the ions can be determined by time-of-flight techniques. For a liquid crystalline material between two ITO coated plates with an initial voltage V_1, a sudden increase in the voltage to V_2 increases the population of electrochemically generated ions, which allows

(36) A larger value of $q = 3.7 \times 10^3$ cm^{-1} ($\beta = 0.018$ rad, $\Lambda = 16.9$ μm) was utilized here versus the beam coupling and the other diffraction efficiency experiments. This was done in order to reduce the grating strength, because eq 4 is not valid for very high diffraction efficiencies. As has been shown previously, the reorientation angle of the director is proportional to $q/(\pi^2L^{-2} + q^2)$.[1,6] This results in a maximum reorientational value at $\Lambda = 2 L = 74$ μm, a value much large than 16.9 μm. Although this is partially offset by a larger E_{sc}, which is proportional to q, the photorefractivity clearly drops for Λ values below 55 μm.[7]
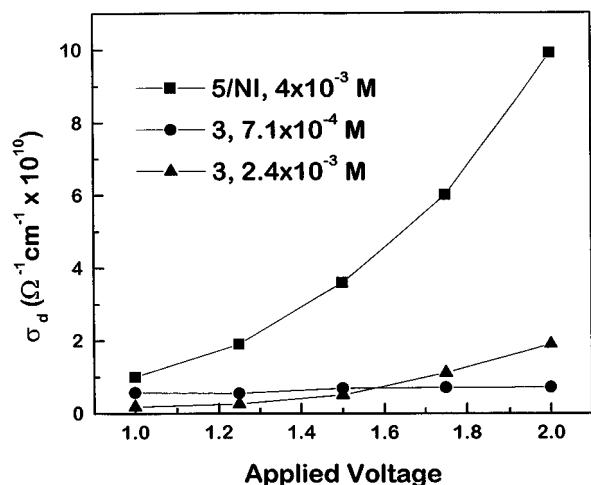
Figure 7. The dark conductivity vs applied voltage is illustrated for samples containing the intermolecular charge transfer dopants **5/NI** and samples containing **3**. The dark conductivity of the **5/NI** sample increases much more steeply with applied voltage. The concentrations of **5** and **NI** are equivalent.

the ionic mean transit time τ_T and the ion mobility to be determined by a modification of the Cottrell equation:[37]

$$i(t) = i_s\left(1 + \left(\frac{V_2}{V_1} - 1\right)e^{(-2t/\tau_T)}\right) \qquad (4)$$

where

$$\tau_T = \frac{2L}{E_A(\mu_+ + \mu_-)} \qquad (5)$$

and where i_s is the saturation current at long times. In order to determine the mobility of the cation, we first studied a sample doped with only **5**. This gave a value for $\tau_T = 17$ s across a 37 μm sample thickness. This yields a value for $\mu_+ = 6.0 \times 10^{-7}$ cm^2 /(V·s). Utilizing $D = \mu k_B T/e_o z$, where z is the charge number, gives a value for $D^+ = 2.7 \times 10^{-8}$ cm^2/s. This value compares favorably to previously determined diffusion coefficients of ions of approximately equal size in liquid crystals.[37] The same experiment for samples doped with **3** gives $\tau_T = 31 \pm 2$ s and $D^+ = 1.5 \times 10^{-8}$ cm^2/s. Using the values of ν for **3** and **5/NI** given above, eq 5 yields $D^- = 2.7 \times 10^{-8}$ cm^2/s for **3** and $D^-(NI^-) = 3.4 \times 10^{-8}$ cm^2/s for **NI**. Thus, in each case the anions are more mobile than the cations.

Redox reactions that occur at the ITO electrodes do not result in serious degradation of the liquid crystal composites.[39] However, they do have the adverse effect of raising the dark current of the composites, which lowers the overall photorefractivity of the materials. Therefore, the fact that the intramolecular dopants require lower cell voltages to achieve a given level of photorefractivity has the added benefit of reducing the dark current. It can be further observed from Figure 7 that the dark conductivity of the intermolecular charge transfer sample increases much more steeply with voltage compared to samples doped with intramolecular charge transfer dopants.

II. Photorefractivity as a Function of Ion-Pair Lifetime. The greater photorefractivity of the intramolecular charge transfer dopants as compared to their intermolecular analogs

can be explained by a mechanism in which the first step following the intramolecular charge separation occurs between the covalent ion pair and a neutral, covalent donor−acceptor pair: $A^+B^- + AB \rightarrow A^+B + AB^-$. Therefore, the longer-lived covalent ion pair clearly leads to an increase in the probability that a collision between it and a neutral covalent donor-acceptor pair will produce an intermolecular charge separation. This intermolecular charge separation is then followed by a second step where either ion diffusion or electron hopping ($AB^- + AB \rightarrow AB + AB^-$) occurs to produce the bulk charge separation that is required to observe the photorefractive effect.

We can quantitatively show that the likelihood of a collision between the ion pairs and neutral donors is far higher than the collision rate between the excited state of **5** and a neutral **NI**. The collision frequency Z can be expressed by the relationship $Z = 8D_{AB}\pi a N_A$, where D_{AB} is the diffusion constant of the neutral dopant, N_A is the number density of the dopant, and a is the radius of the dopant.[33] The diffusion constant D_{AB} is estimated to be equal to the self diffusion constant of the liquid crystal, which is 3×10^{-6} cm^2/s. The radius of the dopant is estimated as half of the length of the dopant, $a \approx 10$ Å. The optimal dopant number density for **3** is 4.3×10^{17} molecules/cm^3. This gives a collision frequency of 3.2×10^6 s^{-1}, or a collision every 0.3 μs. Given that the lifetimes of the charge separated states of **3** and **4** in a liquid crystalline environment are several microseconds (Table 1), approximately 10 collisions during the lifetime of the intramolecular charge separated state are expected to occur. This compares to an excited state lifetime for **5** of 3.5 ns and a collision frequency of **5** with **NI** of 0.35 μs. Therefore, the number of dopant collisions that occur during the ion pair state lifetime of **3** is 1000 times greater than the number of such collisions between **5** and **NI** during the excited state lifetime of **5**.

In order to show that intermolecular charge hopping from the ion pair is thermodynamically possible, we can follow the framework of Suga and Aoyagui, who utilized the collision frequency and Marcus theory to analyze intermolecular electron transfer rates for a reaction scheme of $R_1^- + R_2 \rightarrow R_1 + R_2^-$.[35,40–42] This is directly comparable to the second step of the bulk charge separation process in our liquid crystal, but can be followed for the first step also. The rate of intermolecular charge transfer is given by:

$$k = Z \exp(-E_a/k_B T) \qquad (6)$$

where

$$E_a = \frac{(\Delta G_{CS} + \lambda_T)^2}{4\lambda_T} \qquad (7)$$

$$\lambda_T = \lambda_S + \lambda_i \qquad (8)$$

$$\lambda_S = e_o{}^2\left(\frac{1}{2r_1} + \frac{1}{2r_2} - \frac{1}{r_{12}}\right)\left(\frac{1}{\epsilon_\infty} - \frac{1}{\epsilon_s}\right) \qquad (9)$$

Here, Z is the bimolecular collision rate of the uncharged species, ΔG_{CS} is the free energy for charge separation, λ_T is the total reorganization energy of the solvent (λ_S) and of the

(37) Briere, G.; Herino, R.; Mondon, F. *Mol. Cryst. Liq. Cryst.* **1972**, *19*, 157.

(38) Serra, A. M.; Mariani, R. D.; Abruna, H. D. *J. Electrochem. Soc.* **1986**, *133*, 2226.

(39) Lomax, A.; Hirasawa, R.; Bard, A. J. *J. Electrochem. Soc.* **1972**, *119*, 1679.

(40) Wasielewski, M. R.; Gaines, G. L., III; O'Neil, M. P.; Svec, W. A.; Niemczyk, M. P.; Prodi, L.; Gosztola, D. In *Dynamics and Mechanisms of Photoinduced Transfer and Related Phenomena*; Mataga, N., Okada, T., Masuhara, H., Eds.; Elsevier: New York, 1992.

(41) Marcus, R. A. *J. Chem. Phys.* **1956**, *24*, 966.

(42) Assel, M.; Hofer, T.; Laubereau, A.; Kaiser, W. *Chem. Phys. Lett.* **1995**, *234*, 151.

intramolecular bonds (λ_i), r_1 and r_2 are the radii of the reactants, and r_{12} is the center-to-center distance between the two reactants. For the reaction $A^+B^- + AB \rightarrow A^+B + AB^-$, ΔG_{CS} is derived solely from the loss of Coulomb attraction between A^+ and B^- within A^+B^-, which yields $\Delta G_{CS} = 0.04$ eV. Furthermore, for intermolecular electron transfer, λ_i may be neglected in the estimate of λ_T, leaving λ_S to be estimated.[43] Although eq 11 predicts a value for λ_S of approximately 0.3 eV, Suga and Aoyagui found that their observed reaction rates implied a value for λ_S of approximately one-third the calculated value. This may be due to the fact that the solvent molecules in the neighborhood of the collision are already reorganized to solvate an ion.[29] A value for $\lambda_S = 0.1$ eV produces an initial charge separation reaction rate constant that is 14% of the collision frequency. Given the 3.2×10^6 s^{-1} collision frequency for **3** determined above, the rate constant for the reaction $A^+B^- + AB \rightarrow A^+B + AB^-$ is 4.5×10^5 s^{-1}. For **3** the rate constant for A^+B^- ion pair decay is 2.3×10^5 s^{-1}. Thus, the yield of separated ions is 66%.

For the second step of the bulk charge separation, charge migration can occur through either diffusion or transfer diffusion. The rate of the transfer diffusion can be easily calculated for the reaction $AB^- + AB \rightarrow AB + AB^-$, where $\Delta G_{CS} = 0$.[34] This produces a rate constant for transfer diffusion of:

$$k = Z \exp\left(\frac{-\lambda_T}{4k_B T}\right) \tag{10}$$

Again utilizing $\lambda_S = 0.1$ eV, this produces a transfer diffusion rate constant $k = 1.3 \times 10^6$ s^{-1}. However, since the lifetimes of the AB^- and A^+B ions are at least several seconds based on the lifetimes of the photorefractive gratings, the efficiency of transfer diffusion must be close to unity. Thus, this treatment illustrates that efficient bulk charge separation can occur within liquid crystal composites that possess long-lived intramolecular ion pairs.

III. Lower Concentration Requirements for Intramolecular Dopants. The final observation is that the optimal concentration of samples containing **3** is a factor of 6 less than the composites containing **5/NI**. Furthermore, the photorefractivity of the **5/NI** composites increases monotonically with dopant concentration and is limited only by solubility. This is in contrast to the composites containing **3**, where photorefractivity is found to be optimized for concentrations of only 1×10^{-3} M. These observations are a consequence of the differences in the mechanisms for producing bulk charge separation between the intramolecular and intermolecular dopants that are elaborated

in section II of the Discussion. As illustrated in Scheme 1,[42,43] in order for mobile charge generation to occur in samples containing **5/NI**, an optically excited **5** must undergo a collision with **NI**. Therefore, the rate of charge transfer is ultimately limited by the concentration of NI, which alters the reaction rate constant for the initial charge separation, $k_{CS} = 1/([NI]\tau_{CS})$. Given the short excited state lifetime of **5**, this relationship shows that the **5/NI** system is limited by the bimolecular collision rate and explains the monotonic increase of photorefractivity with an increase in the concentration of dopants for this system. This contrasts with the intramolecular charge transfer dopants discussed in section II, where bulk charge separation is no longer limited by the collision frequency, but by the lifetime of the initial intramolecular ion pair state.

The limiting factor for the photorefractivity of composites containing **3** appears to be a sharp rise in the dark conductivity. This is illustrated in Figure 7 for two concentrations of dopant **3**. The larger concentration clearly begins to show enhanced dark conductivity as a function of voltage, whereas the optimal concentration shows no increase in dark conductivity. This is presumably due to enhanced electrochemical activity for higher concentration samples at the ITO interface, which produces lower photorefractivity through higher dark currents.

Conclusions

We have induced large photorefractive grating diffraction efficiencies in nematic liquid crystals by doping them with molecules that undergo intramolecular charge separation. The intramolecular charge transfer dopants are shown to be superior for inducing photorefractivity relative to identical electron donors and acceptors which must undergo intermolecular charge separation. This is shown to be a result of several factors. The first is the larger difference between the magnitude of the diffusion coefficients of the cation and anion for the intramolecular charge transfer dopants relative to the intermolecular dopants. It is also shown that the magnitude of the photorefractive effect increases with longer ion pair lifetimes for the intramolecular charge transfer dopants. This is consistent with Marcus theory and transfer diffusion theory, which describes bulk charge migration through charge hopping between donor–acceptor molecules. The greater efficiency of mobile charge generation for the intramolecular charge transfer dopants permits the use of lower concentrations and reduced absorption of the samples.

(43) Gould, I. R.; Ege, D.; Moser, J. E.; Farid, S. *J. Am. Chem. Soc.* **1990**, *112*, 4290.